and 100%, respectively (Table I). Addition of the initiators to preformed products did not cause isomerization of the alkenyl group, and, further, addition of hydroquinone in reaction 4 decreased the percentage of the *trans*-alkenyl product (Table I).

The involvement of free radicals was strongly suggested by the detection of spin adducts using phenyl-*N*-*tert*-butylnitrone (PBN) as spin trap.[5] Typically, the ESR experiment was conducted by adding deoxygenated benzene to a silica tube fitted with a serum cap and containing weighed amounts of PBN and I. DMA was then introduced through the serum cap to give final concentrations of PBN, I, and DMA of 0.1, 0.1 and 0.16 M, respectively. The very weak ESR signal observed at room temperature increased in intensity >10 times after the reaction mixture had been heated to 70 °C for 10 min. The same ESR signal (in addition to that of the butoxy adduct[6]) could be observed at room temperature if a small amount of DBPO was present (~5% mol ratio). The ESR signal (Figure 1a) shows no change in the relative intensities of the peaks over a period of >4 days and is apparently due to only one species. A computer-simulated spectrum with hyperfine constants A_N = 14.32, A_H = 4.1, and A_{Pt} = 6.6 G (g = 2.013) agrees well (Figure 1b) with the observed spectrum.

In the absence of either DMA or I, no spin adduct was observed,[7] nor was an ESR signal observed when I was replaced in the reaction by *trans*-$PtCl_2(PEt_3)_2$. However, the magnitudes of the various hyperfine splittings are affected by the anionic ligand (for NO_3^- g = 2.013, A_N = 14.31 G, A_H = 4.3 G, A_{Pt} = 4.9 G) and also by the acetylene used (for $CH_3C{\equiv}CCOOCH_3$ g = 2.013, A_N = 14.58 G, A_H = 4.3 G, A_{Pt} = 5.2 G).[8] Thus the trapped platinum radical has the formula ·$PtCl(PEt_3)_2$(acetylene), a formally Pt(I) species and the spin adduct is

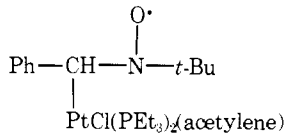

It must be emphasized that the platinum radical identified in the trapping experiments probably plays an important role in the actual insertion process since, in the presence of initiators and more importantly in the thermal reaction, increased yields of the trans vinylic product are always paralleled by observed increases (by ESR) in the concentration of the radical. Moreover, when I is allowed to react with DMA (0.5 molar equiv) in 2-butyne as solvent (ratio of DMA to 2-butyne 1:100), at room temperature with 5% DBPO added, only the DMA insertion products are formed, leaving unreacted **I**. Apparently, it is essential to first form a five-coordinate acetylene–platinum complex, from which the platinum-containing radical is then generated.

Further, since in reaction 4 conducted with DBPO added the percentage of the *trans*-alkenyl product (100%) obviously exceeds the amount of radical initiator added (5%), the reaction must also proceed via a chain mechanism.[9] The absence of any detectable amount of *cis*-alkenyl isomer implies that (a) the free-radical mechanism dominates the reaction, and (b) the radical reaction is highly stereospecific. A mechanism consistent with these observations is depicted in eq 5–8.

$$PtHCl(PEt_3)_2 + DMA \rightleftharpoons PtHCl(PEt_3)_2(DMA) \quad (5)$$

$$\underset{\text{initiator}}{\text{In}\cdot} + PtHCl(PEt_3)_2(DMA) \rightarrow InH + \text{IIIa} \quad (6)$$

$$\text{IIIa} \rightleftharpoons \text{IIIb} \rightleftharpoons \text{IIIc} \quad (7)$$

$$\text{IIIc} + PtHCl(PEt_3)_2(DMA) \rightarrow PtCl(DMAH)(PEt_3)_2 + \text{IIIa} \quad (8)$$

The stereospecificity at the alkenyl bond is thought to be due to the fact that only IIIc has the ability to abstract H· from $PtHCl(PEt_3)_2$(DMA). Molecular models suggest that in this complex the H atom on Pt is so well shielded by the phosphine ethyl groups making abstraction by IIIb sterically unfavorable.

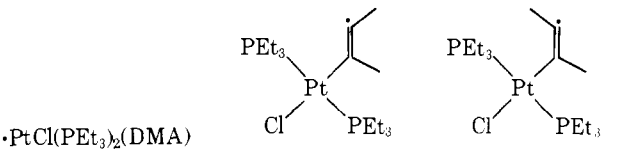

·$PtCl(PEt_3)_2$(DMA) IIIa — *cis*- or *trans*-IIIb — *cis*- or *trans*- IIIc

In the thermal reaction initiation may involve hydrogen abstraction by a second acetylene (eq 9).

$$PtHCl(PEt_3)_2(DMA) + DMA \xrightarrow{\Delta} DMAH\cdot + \cdot PtCl(PEt_3)_2(DMA) \quad (9)$$

IIIa

These results provide the first evidence of free-radical participation in acetylene insertions into transition metal hydrides, although related radical reactions have been described previously.[10,11] In view of current interest in the stereochemistry[12] of acetylene insertions into the metal–hydrogen bond, and in view of the high stereospecificity observed in this reaction, the possible involvement of free-radical addition in other stereospecific trans addition reactions should not be discounted.

Acknowledgments. Special thanks are due to Dr. S. K. Wong, Dr. E. G. Janzen, and Mr. E. R. Davis for helpful discussions and experimental assistance. The continued financial support of the National Research Council of Canada is gratefully acknowledged.

References and Notes

(1) T. G. Attig, H. C. Clark, and C. S. Wong, *Can. J. Chem.*, **55**, 189 (1977), and references therein.
(2) The first prefix refers to the geometry at platinum, the second refers to geometry about the double bond.
(3) The various isomers were fully characterized by elemental analysis, melting point, and ^1H and ^{31}P spectra (see ref 1).
(4) Control experiments at 70 °C showed no isomerization of the alkenyl group, and only slow cis to trans isomerization at Pt.
(5) E. G. Janzen, *Acc. Chem. Res.*, **4**, 31 (1971).
(6) The butoxy adduct decomposes more rapidly so that, after 2 days, the ESR spectrum is identical with that obtained by thermal generation of the radicals.
(7) Although a mixture of PBN and DMA does not exhibit any ESR signal, PBN being a zwitterion does induce polymerization of DMA.
(8) Compound I reacted with $CH_3C{\equiv}CCOOCH_3$ in benzene, with DBPO added, to give the vinylic insertion product in >50% yield.
(9) Reaction 4 in the presence of DBPO is exothermic and is complete within an hour (cf. days of reaction time in the absence of initiator).
(10) T. G. Appleton, M. H. Chisholm, H. C. Clark, and K. Yasufuku, *J. Am. Chem. Soc.*, **96**, 6600, (1974).
(11) N. G. Hargreaves, R. J. Puddephatt, L. H. Sutcliffe, and P. J. Thompson, *J. Chem. Soc., Chem. Commun.*, 861 (1973).
(12) See, for example, S. Otsuka and A. Nakamura, *Adv. Organomet. Chem.*, **14**, 245, (1976).

H. C. Clark,* C. S. Wong
Guelph–Waterloo Centre for Graduate Work in Chemistry
Guelph Campus, Chemistry Department
University of Guelph, Guelph, Ontario, Canada N1G 2W1
Received May 31, 1977

Encapsulation of Hydrogen in Molecular Sieve Zeolites

Sir:

Recent interest in the use of hydrogen as a multipurpose fuel[1] has emphasized the necessity of a reliable storage system for this element. Among various methods previously suggested, storage as metal hydride seems the most promising.[2] Thus,

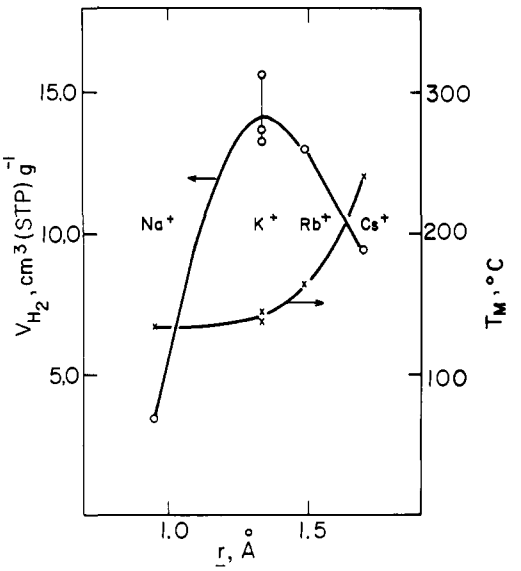

Figure 1. Change in V_{H_2} (O plot) and T_M (× plot) of A-type zeolites as a function of the radius of exchangeable alkali cation (temperature, 300 °C; pressure, 1300 psi; loading time, 15 min).

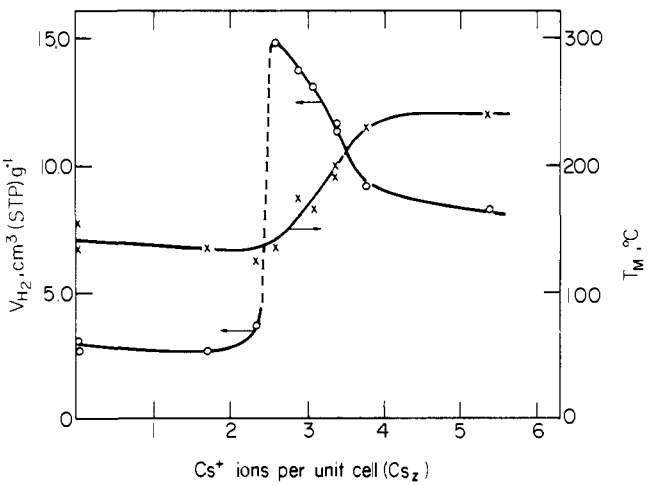

Figure 2. Change in V_{H_2} (O plot) and T_M (× plot) of CsNaA-type zeolite as a function of Cs_z (pressure, 1200 psi; temperature and loading time as in Figure 1).

$LaNi_5$ alloy stores up to 1.6%, while FeTi ~1% by wt of hydrogen.[3,4] We have now developed an alternative approach to this problem, i.e., hydrogen encapsulation in molecular sieves. The method is related to some previous work on the possibility of encapsulating inert gases in natural and synthetic zeolites.[5,6]

It was found in the present study that appropriately exchanged zeolites, in particular CsA-type zeolite, can be used as efficient media for hydrogen encapsulation.[7] The latter was performed at 200–400 °C, in the pressure range of 350–13 300 psi, using loading times of 15–90 min. Experiments were run in a pressure vessel, connected to a hydrogen source and a high pressure gauge. The system was also equipped with a high vacuum line. Zeolite samples were freshly activated (16 h at 450 °C, under air) and thoroughly outgassed (>1 h at 300 °C, 10^{-5} Torr) before being subjected to the selected encapsulation pressure and temperature. After quenching to 25 °C, and subsequent release of excess pressure, the encapsulate was evacuated to remove adsorbed hydrogen. Release of encapsulated hydrogen was then carried out by heating the sample at a constant rate of 10°/min, up to the encapsulation temperature. The amount of hydrogen released was followed and determined in terms of the pressure developed in a calibrated volume, converted into cubic centimeter per gram of zeolite at STP. The total amount of gas released was defined as the maximal hydrogen encapsulation capacity (V_{H_2}) of the zeolite. Using the TPD method,[8] temperatures of maximal rate of hydrogen release, T_M, were derived in order to evaluate the thermal stability of the encapsulate. Unless otherwise specified, the encapsulation experiments were found to be fully reproducible, and to cause no damage to the zeolite structure, as confirmed by x-ray crystallographic analysis.

Results obtained are summarized in Figures 1, 2 and 4. The encapsulation efficiency of A-type zeolites, in terms of V_{H_2} and T_M, is plotted in Figure 1 as a function of the size of the exchangeable alkali cation.[9] As seen, V_{H_2} increases with increase in ionic radius (r) from Na^+ to K^+ but then decreases for the larger (Rb^+ and Cs^+) ions. The observed dependence is probably the resultant of two opposing factors determining the V_{H_2} value; i.e., with increase in r the effective critical pore size decreases, hence encapsulate stability (T_M) increases, while, on the other hand, available intracrystalline void volume per gram of zeolite decreases. For K-A zeolite reproducibility is rather poor, and, unlike all other cases, the V_{H_2} value is dependent on the efficiency of evacuation, preceding the hydrogen release. It is found that after 45 h at 25 °C the K-A(H_2) encapsulate loses 46% of its hydrogen. In contrast, Cs-A shows after 5 days a decrease in V_{H_2} of only 7%. This indicates that in spite of their somewhat lower capacities Cs-A and Rb-A are markedly better hydrogen encapsulants.

In Figure 2 the V_{H_2} and T_M values for CsNaA-type zeolite are plotted as a function of the number of Cs^+ ions per unit cell (Cs_z).[9] As seen, encapsulation capacity remains essentially unchanged for Cs_z values up to ~2, but then, at $Cs_z = 2.5$ the V_{H_2} value shows a sharp (5.5-fold) jump. Further increase in Cs_z results in gradual decrease in V_{H_2} until a stable value is reached at $Cs_z \sim 5.5$. The T_M curve shows a plateau in the Cs_z range of 0–2.5, and another, higher plateau for $Cs_z > 4$. These observations can be rationalized by considering the anticipated structural changes in A-type zeolite with the progress of the $Na^+ \rightarrow Cs^+$ exchange. In the original Na-A zeolite diffusion of hydrogen molecules (kinetic diameter, $\sigma = 2.89$ Å) through the main channel system is essentially free, since Na^+ in II sites does not effectively block the 8-ring apertures (4.2 Å) interconnecting the α cages.[10] Consequently, encapsulation is restricted to the β cages, representing ~17% of the total void volume. As Na^+ ($r = 0.95$ Å) is gradually replaced by Cs^+ ($r = 1.69$ Å) in II sites, the 8-ring apertures become blocked, causing hydrogen encapsulation in α cages. At $Cs_z = 3.0$, corresponding to complete Cs^+ occupation of the II sites,[7] all α cages should become effectively closed for hydrogen diffusion at ambient temperature with consequent sharp increase in V_{H_2}. However, it is found that the anticipated increase occurs already at $Cs_z = 2.5$ (Figure 2), corresponding to Cs^+ exchange in five out of the six possible II sites in a unit cell. This finding is in excellent agreement with the percolation theory[11] and previously reported results of a cut-off in the sorption of nonpolar gases in exchanged A zeolites, having ~2.5 blocked octagonal windows per unit cell.[12,13] At this point there is only one open 8 ring left in a unit cell and, consequently, percolation through the main channel is prevented. At $Cs_z > 3$, as Cs^+ gradually replaces Na^+ in I sites, V_{H_2} decreases until a nearly constant value is reached at $Cs_z \sim 5.5$. This decrease is larger than anticipated by considering only the decrease in available void volume in the 3–5.5-Cs_z region, and may depend on some additional, so far undetermined, factors. The T_M low constant value (135 °C) for Cs_z up to 2.5 is apparently related to activated diffusion from β cages, while the high constant value (240 °C) at $Cs_z > 4$ is probably due to activated diffusion from Cs^+-blocked α cages.

Figure 3 shows a simplified model[14] for the hydrogen encapsulate of Cs_3Na_9A zeolite.[12] Each β cage, with a void vol-

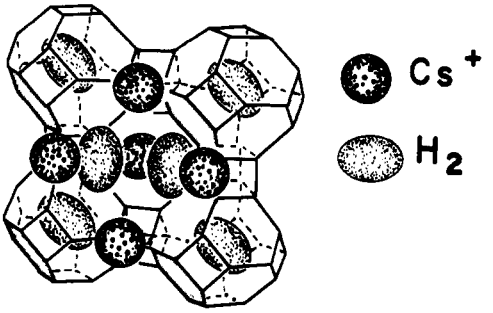

Figure 3. Proposed model for the hydrogen encapsulate of Cs_3Na_9A-type zeolite (Cs_{II}^+ indicated; Na_I^+ omitted).

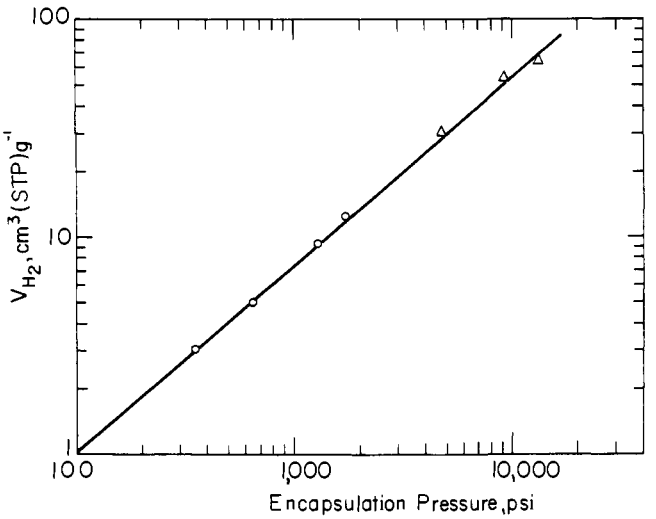

Figure 4. Dependence of V_{H_2} upon the encapsulation pressure at 300 °C (○, lower region; △, higher region of measurement).

ume of 155 Å^3, and each α cage, with a gross empty volume of 775 Å^3, could admit a variable number of hydrogen molecules depending on the encapsulation conditions. The change in encapsulation capacity of $Cs_{5.4}Na_{6.6}A$ (Cs_z = 5.4) with pressure is shown in Figure 4. A deviation from linear dependence of V_{H_2} upon the encapsulation pressure (p) is observed, and the empirical expression $V_{H_2} = 0.017\,p^{0.868}$, derived from the graph, holds both for the low (300–1700 psi) and the high (4000–13 300 psi) regions of measurements. At 13 300 psi, V_{H_2} = 65 cm^3 (STP) g^{-1}, corresponding to 0.6% by weight. The results obtained are in good agreement with the van der Waals equation for real gases, indicating that the stability of the Cs-A(H_2) encapsulate remains entirely unaffected by the encapsulation pressure up to 13 000 psi, and that V_{H_2} values >1% at higher pressures are feasible. This, coupled with the possibility of temperature-controlled slow release of the element, illustrates the potential importance of the principle of hydrogen encapsulation in energy and related problems.

Acknowledgment. This project was sponsored and allowed for publication by the Office of the Chief Scientist, The Ministry of Commerce and Industry, Israel. Thanks are due to Dr. I. Lewkowicz for permission to use the high pressure equipment at Soreq Nuclear Research Center, Yavne, Israel.

References and Notes

(1) D. P. Gregory, *Sci. Am.*, **228**, 13 (1973); C. A. McAuliffe, *Chem. Ind. (London)*, 725 (1975); *Chem. Br.*, **9**, 559 (1973); T. N. Veziroglu, "Hydrogen Energy", Plenum Press, New York, N.Y., 1975.
(2) D. L. Cummings and G. J. Powers, *Ind. Eng. Chem., Process Des. Dev.*, **13**, 182 (1974).
(3) J. H. N. Van Vucht, F. A. Kuijpers, and H. C. A. M. Bruning, *Philips Res. Rep.*, **25**, 133 (1970).
(4) J. J. Reilly and J. R. Johnson, *Proc. World Hydrogen Energy Conf., 1st, 1976*, II, paper 8B-3 (1976).
(5) W. J. Sesny and L. H. Shaffer, U. S. Patent 3 316 691 (1967).
(6) R. M. Barrer and D. E. W. Vaughan, *Trans. Faraday Soc.*, **67**, 2129 (1971), and references therein.
(7) The aluminosilicate framework of A-type zeolite is characterized by two types of polyhedra, i.e., an α cage (26-hedron of type I) and a β cage (14-hedron of type I).[10] The main intracrystalline channel system is formed by interconnection of α cages through 8 rings (d = 4.2 Å). The structure is cubic, and each α cage is connected to eight β cages through 6 rings (d = 2.2 Å). In the dehydrated, alkali-exchanged zeolite there are twelve cations per pseudocell, eight of them near the center of 6 rings (site I) and three near the 8 rings (site II). The exact dimensions of these ring apertures depend on the size of the cations in sites I and II, and, consequently, guest molecules can penetrate the α or β cages only if their kinetic diameter (σ) is smaller than the effective apertures. However, if σ is only slightly bigger than the aperture, guest molecules can be forced into the cavities by applying high pressure and elevated temperature. Quenching to room temperature results in trapping (encapsulation) of the molecules inside the cavities. The process can be reversed and the trapped molecules can be released upon heating the zeolite.
(8) Y. Amenomiya, *Chem. Tech.*, **6**, 128 (1976).
(9) The extent of ion exchange, as determined by atomic absorption and/or flame emission analysis, was 72% for K-A, 46% for Rb-A, and 45% for Cs-A, corresponding to the formulae $K_{8.6}Na_{3.4}$-A, $Rb_{5.5}Na_{6.5}$-A, and $Cs_{5.4}Na_{6.6}$-A, respectively; 0.4 M (CsCl + NaCl) solutions, containing variable relative concentrations of the two salts, were used to prepare CsNa-A samples with various Cs_z (Figure 2).
(10) D. W. Breck, "Zeolite Molecular Sieves", Wiley, New York, N.Y., 1974, pp 83–90.
(11) J. M. Hammersley and D. C. Handscomb, "Monte Carlo Methods", Methuen, London, 1964, Chapter 11, p 158.
(12) L. V. C. Rees and T. Berry, *Proc. Conf. Mol. Sieves, 1969*, 149 (1969).
(13) T. Takaishi, Y. Yatsurugi, A. Yusa, and T. Kuratomi, *J. Chem. Soc., Faraday Trans. 1*, **71**, 97 (1975); T. Takaishi, T. Ogushi, and A. Yusa, *Int. Conf. Mol. Sieves, 4th, 1977*, 95 (1977).
(14) This model is drawn after the array of 14-hedra in zeolite A.[10] It shows a "half" of an α cage surrounded by four β cages. The exact position of the H_2 molecules is unknown, and their number (5 per unit cell, corresponding to ~0.5% by weight) was chosen arbitrarily.
(15) K. Seff, *Acc. Chem. Res.*, **9**, 121 (1976).
(16) Research Associate.

Dan Fraenkel,[16] Joseph Shabtai*
Department of Organic Chemistry
The Weizmann Institute of Science, Rehovot, Israel
Received April 13, 1977

The First Formally Three-Coordinate d^8 Complex: Tris(triphenylphosphine)rhodium(I) Perchlorate and Its Novel Structure

Sir:

Kinetic studies indicate that an unisolable three-coordinate d^8 compound of rhodium(I), $RhCl(PPh_3)_2$, formed dissociatively from $RhCl(PPh_3)_3$, is the raison d'être of Wilkinson's catalyst in the homogeneous hydrogenation of alkenes.[1] Thus, the successful synthesis and isolation of any three-coordinate d^8 complex would not only corroborate their previously doubted existence as intermediates but hold promise of high reactivity and considerable catalytic potential. Moreover, a very interesting structural dilemma is anticipated for d^8 metals with two vacant coordination sites. The steric predilection of three bulky ligands for trigonal planarity would mandate paramagnetism,[2] but the prevailing diamagnetism of low-valent phosphine complexes (of even d^n configuration) makes this highly unlikely. Group 8 complexes with two sites of coordinative unsaturation (so-called 14-electron compounds) are known only in a d^{10} configuration, exemplified by ML_2 complexes of the nickel triad, and show expected linear coordination.[3]

Synthetic routes to complexes of unusually low coordination number have exploited bulky phosphines,[3] sterically demanding anions,[4] and dilute low temperature matrices.[5] Our strategy has been to employ bulky phosphines under conditions which remove potentially bridging anions and donor solvents. Treatment of $RhCl(PPh_3)_3$ with $TlClO_4$ in donor solvents such as acetone, ethers, or alcohols precipitates the halide as TlCl allowing isolation of the orange crystalline complexes $[Rh(solvent)(PPh_3)_3]ClO_4$ (**1**). Evidence such as the low ν_{CO} (1665 cm^{-1}) in the acetone complex indicates that these